Inorg. Chem. **2008**, *47*, 1476−1487

Highly Phosphorescent Iridium Complexes with Chromophoric 2-(2-Hydroxyphenyl)oxazole-Based Ancillary Ligands: Interligand Energy-Harvesting Phosphorescence

Youngmin You,[†] Jangwon Seo,[†] Se Hun Kim,[‡] Kil Suk Kim,[§] Tae Kyu Ahn,[§] Dongho Kim,*[,§] and Soo Young Park*[,†]

Department of Materials Science & Engineering, Seoul National University, San 56-1, Shillim-Dong, Kwanak-Gu, Seoul 151-744, Korea, Pyungtaek R&D Center, Dongwoo FineChem Co., Ltd., 1177, Pyungtaek-Si, Kyunggi-Do, 451-764, Korea, and The Center for Ultrafast Optical Characteristics Control and Department of Chemistry, Yonsei University, Seoul 120-749, Korea

Received September 10, 2007

We disclose a controlled phosphorescence color tuning in a series of cyclometalated heteroleptic Ir(III) complexes (Ir(III) bis(2-(2,4-difluorophenyl)pyridinato-*C,N*$^{2'}$)(LX)) containing chromophoric 2-(2-hydroxyphenyl)oxazole-derivative ancillary ligands (LX). From a cyclometalated chloride-bridged Ir(III) dimer, three highly emissive cyclometalated heteroleptic Ir(III) complexes were obtained in good yields, each with a different conjugative plane in the chromophoric ancillary ligand (i.e., 2-(2-hydroxyphenyl)-4-methyloxazole, 2-(2-hydroxyphenyl)-6-methylbenzoxazole, and 2-(2-hydroxyphenyl)naphthoxazole). The three Ir(III) complexes showed highly efficient greenish blue (500 nm), green (525 nm), and yellow (552 nm) phosphorescence, respectively; a regular ca. 0.11 eV bathochromic shift was observed for each additional phenyl ring fused to the oxazole ring in the ancillary ligand. From the absorption, electrochemical measurements, static and transient photoluminescence (PL), and time-dependent density functional theory (TD-DFT) calculations, it can be concluded that the Ir(III) complexes have a single emission center with dual excitation paths. Finally, this characteristic energy-harvesting phosphorescence was further demonstrated in electrophosphorescence devices.

Introduction

Phosphorescent transition metal complexes have attracted significant attention on account of their potential uses in various optoelectronic applications. The use of these complexes as emitting materials in organic light-emitting devices (OLEDs) is particularly beneficial because, theoretically, 100% internal quantum efficiency can be attained by utilizing both triplet and singlet excitons through the strong spin–orbit coupling provided by the core atom.[1] In this regard, considerable effort has been devoted to finding transition metal complexes suitable for OLED applications. These studies have identified congeners with a d^6 metal atom such as Ru(II),[2a–d] Os(II),[2e–g] or Ir(III)[2h–r] as the core atom having particular promise. Among the complexes studied to date, cyclometalated trischelated Ir(III) complexes have emerged as particularly promising candidate materials since the pioneering works carried out by the group of Thompson and Forrest.[3] The very high phosphorescence quantum efficiency and relatively short phosphorescence lifetime (several microseconds) of Ir(III) complexes enable high efficiency electrophosphorescence. Extensive synthetic studies have been carried out with a view to developing Ir(III) complexes with improved characteristics, in particular saturated phosphorescence color, high phosphorescence efficiency, and physical compatibility.[4] Particularly, well-defined molecular design methods for efficient phosphorescence color tuning are currently under active investigation with the aim of achieving full-color displays.

* To whom correspondence should be addressed. E-mail: parksy@snu.ac.kr (S.Y.P.), dongho@yonsei.ac.kr (D.K.).
[†] Seoul National University.
[‡] Dongwoo FineChem Co.
[§] Yonsei University.

(1) (a) Baldo, M. A.; O'Brian, D. F.; You, Y.; Shoustikov, A.; Sibley, S.; Thompson, M. E.; Forrest, S. R. *Nature* **1998**, *395*, 151–154. (b) Baldo, M. A.; Lamansky, S.; Burrows, P. E.; Thompson, M. E.; Forrest, S. R. *Appl. Phys. Lett.* **1999**, *75*, 4–6. (c) Ikai, M.; Tokito, S.; Sakamoto, Y.; Suzuki, T.; Taga, Y. *Appl. Phys. Lett.* **2001**, *79*, 156–158. (d) Chen, F. C.; Yang, Y.; Thompson, M. E.; Kido, J. *Appl. Phys. Lett.* **2002**, *80*, 2308–2310. (e) Baldo, M. A.; Thompson, M. E.; Forrest, M. E. *Nature* **2000**, *403*, 750–753.

10.1021/ic701778f CCC: $40.75
Published on Web 02/07/2008

Chart 1. Schematic representation of the photophysical process of phosphorescent Ir(III) complexes (C^N cyclometalating ligand; LX ancillary ligand; ISC intersystem crossing)

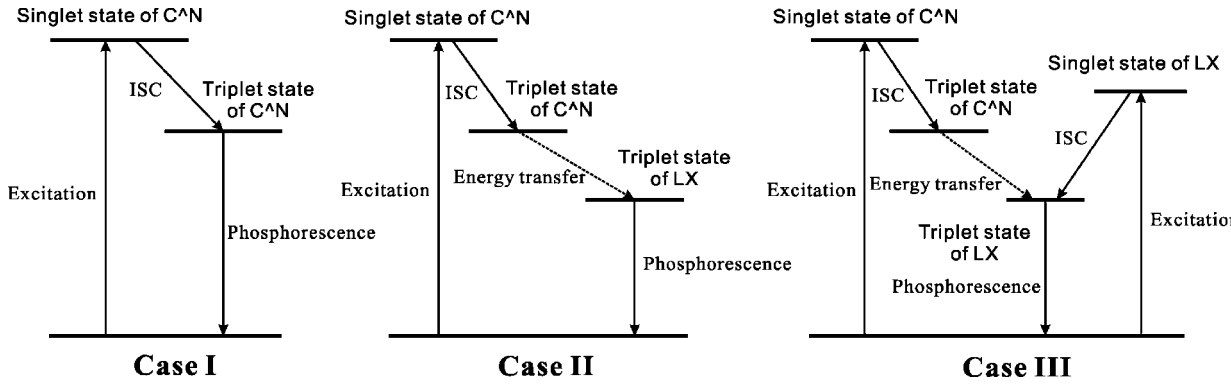

A trischelated neutral Ir(III) complex consists of three monoanionic bidentate ligands and a core Ir atom. Such complexes are called "homoleptic" if the three ligands are identical or "heteroleptic" if the ligands are not identical. Usually, heteroleptic Ir(III) complexes comprise two cyclometalating ligands (C^N), such as 2-phenylpyridine (ppy), and one ancillary ligand (LX). In general, the triplet emission of Ir(III) complexes, either homoleptic or heteroleptic, is generated from the metal to the cyclometalating ligand charge-transfer (ML_CCT) transition state or the cyclometalating ligand centered (L_CC) transition state. For both of these transition pathways, however, it is considered that the lowest unoccupied molecular orbital (LUMO) is located over the cyclometalating ligand (Chart 1, case I).[5] Therefore, the phosphorescence color tuning of both homoleptic and heteroleptic Ir(III) complexes has been mainly explored through structural investigations of cyclometalating ligands,[4a,c,f,g,6] with little attention being devoted to the ancillary ligands (LX), which play an insignificant role in phosphorescence and only act as *ancillary* reactants for the final complexes. However, the design and synthesis of Ir(III) complexes containing new cyclometalating ligands are frequently limited by unfavorable side reactions and steric crowding around the Ir(III) center. Furthermore, because we can only obtain singly emissive Ir(III) complexes from one cyclometalating ligand, this methodology (i.e., modifying the structure of the cyclometalating ligand) is a rather inefficient approach to color tuning.

An alternative approach to phosphorescence color tuning is to use *chromophoric* ancillary ligands. Several groups have reported facile and efficient color tuning by employing heteroleptic Ir(III) complexes containing such ancillary ligands: Kwon et al. investigated the color tuning effect of quinoline carboxylate and isoquinoline carboxylate chromophoric ancillary ligands,[7a] and Kappaun et al. observed significant phosphorescence color changes with 8-quinolinolate chromophoric ancillary ligands.[7b] In addition, we previously showed that pyridylcarboxylate ancillary ligands could be used to effectively modulate the phosphorescence color across the full visible range.[7c,d] In these Ir(III) complexes, both a cyclometalating ligand with a higher triplet state energy and an ancillary ligand with a lower triplet state energy were coordinated to the Ir(III) core to make a heteroleptic complex. For this class of Ir(III) complexes, we directly observed that excitation of the cyclometalating ligand was followed by highly efficient interligand energy transfer (ILET) to the ancillary ligand, which eventually provided an ancillary ligand centered color-tuned phosphorescence. In our study of these complexes, however, we observed no significant differences among the absorption spectra of the complexes even though various ancillary ligands were employed. On the basis of this observation, we tentatively

(2) (a) Tung, Y.-L.; Lee, S.-W.; Chi, Y.; Chen, L.-S.; Shu, C.-F.; Wu, F.-I.; Carthy, A. J.; Chou, P.-T.; Peng, S.-M.; Lee, G.-H. *Adv. Mater.* **2005**, *17*, 1059–1064. (b) Liu, C.-Y.; Bard, A. J. *J. Am. Chem. Soc.* **2002**, *124*, 4190–4191. (c) Barron, J. A.; Bernhard, S.; Houston, P. L.; Abruna, H. D.; Ruglovsky, J. L.; Malliaras, G. G. *J. Phys. Chem. A* **2003**, *107*, 8130–8133. (d) Rudmann, H.; Shimada, S.; Rubner, M. F. *J. Am. Chem. Soc.* **2002**, *124*, 4918–4921. (e) Tung, Y.-L.; Wu P.-C.; Liu, C.-S.; Chi, Y.; Yu, J.-K.; Hu, Y.-H.; Chou, P.-T.; Peng, S.-M.; Lee, G.-H.; Tao, Y.; Carthy, A. J.; Shu, C.-F.; Wu, F.-I. *Organometallics* **2004**, *23*, 3745–3748. (f) Cunningham, G. B.; Li, Y.; Liu, S.; Schanze, K. S. *J. Phys. Chem. B* **2003**, *107*, 12569–12572. (g) Gao, F. G.; Bard, A. J. *Chem. Mater.* **2002**, *14*, 3465–3470. (h) He, G.; Schneider, O.; Qin, D.; Zhou, X.; Pfeiffer, M.; Leo, K. J. *Appl. Phys.* **2004**, *95*, 5773–5777. (i) Gong, X.; Robinson, M. R.; Ostrowski, J. C.; Moses, D.; Bazan, G. C.; Heeger, A. J. *Adv. Mater.* **2002**, *14*, 581–585. (j) Jiang, C.; Yang, W.; Peng, J.; Xiao, S.; Cao, Y. *Adv. Mater.* **2004**, *16*, 537–541. (k) Ramos-Ortiz, G.; Oki, Y.; Kippelen, B. *Phys. Chem. Chem. Phys.* **2002**, *4*, 4109–4114. (l) Yang, X. H.; Neher, D. *Appl. Phys. Lett.* **2004**, *84*, 2476–2478. (m) Zhu, W.; Mo, Y.; Yuan, M.; Yang, W.; Cao, Y. *Appl. Phys. Lett.* **2002**, *80*, 2045–2047. (n) Lee, C.-L.; Lee, K. B.; Kim, J.-J. *Appl. Phys. Lett.* **2000**, *77*, 2280–2282. (o) Coppo, P.; Duati, M.; Kozhevnikov, V. N.; Hofstraat, J. W.; De Cola, L. *Angew. Chem., Int. Ed.* **2005**, *44*, 1806–1810. (p) Plummer, E. A.; van Diken, A.; Hofstraat, H. W.; De Cola, L.; Brunner, K. *Adv. Funct. Mater.* **2005**, *15*, 281–289. (q) Slinker, J. D.; Koh, C. Y.; Malliaras, G. G.; Lowry, M. S.; Bernhard, S. *Appl. Phys. Lett.* **2005**, *86*, 173506–173508. (r) Liu, H.-M.; He, J.; Wang, P.-F.; Xie, H.-Z.; Zhang, X.-H.; Lee, C.-S.; Sun, B.-Q.; Xia, Y.-J. *Appl. Phys. Lett.* **2005**, *87*, 221103–221105.

(3) (a) Lamansky, S.; Djurovich, P.; Murphy, D.; Adbel-Razzaq, F.; Lee, H.-E.; Adachi, C.; Burrows, P. E.; Forrest, S. R.; Thompson, M. E. *J. Am. Chem. Soc.* **2001**, *123*, 4304–4312. (b) Lamansky, S.; Kwong, R. C.; Nugent, M.; Djurovich, P. I.; Thompson, M. E. *Org. Electron.* **2001**, *2*, 53–62. (c) Kawamura, Y.; Yanagida, S.; Forrest, S. R. J. *Appl. Phys.* **2002**, *92*, 87–93. (d) Adachi, C.; Kwong, R. C.; Djurovich, P.; Adamovich, V.; Baldo, M. A.; Thompson, M. E.; Forrest, M. E. *Appl. Phys. Lett.* **2001**, *79*, 2082–2084. (e) Lamansky, S.; Djurovich, P. I.; Abdel-Razzaq, F.; Garon, S.; Murphy, D. L.; Thompson, M. E. *J. Appl. Phys.* **2002**, *92*, 1570–1575. (f) Adachi, C.; Lamansky, S.; Baldo, M. A.; Kwong, R. C.; Thompson, M. E.; Forrest, S. R. *Appl. Phys. Lett.* **2001**, *78*, 1622–1624. (g) Lamansky, S.; Djurovich, P.; Murphy, D.; Abdel-Razzaq, F.; Kwong, R.; Tsyba, I.; Bortz, M.; Mui, B.; Bau, R.; Thompson, M. E. *Inorg. Chem.* **2001**, *40*, 1704–1711. (h) Tamayo, A. B.; Alleyne, B. D.; Djurovich, P. I.; Lamansky, S.; Tsyba, I.; Ho, N. N.; Bau, R.; Thompson, M. E. *J. Am. Chem. Soc.* **2003**, *125*, 7377–7387. (i) Sajoto, T.; Djurovich, P. I.; Tamayo, A.; Yousufuddin, M.; Bau, R.; Thompson, M. E.; Holmes, R. J.; Forrest, S. R. *Inorg. Chem.* **2005**, *44*, 7992–8003. (j) Li, J.; Djurovich, P. I.; Alleyne, B. D.; Yousufuddin, M.; Ho, N. N.; Thomas, J. C.; Peters, J. C.; Bau, R.; Thompson, M. E. *Inorg. Chem.* **2005**, *44*, 1713–1727.

concluded that the phosphorescence was initiated through excitation of the cyclometalating ligand and that direct excitation of the ancillary ligand was not involved in this initial step (Chart 1, case II). As part of our ongoing efforts to generalize this unique phosphorescence color tuning methodology, here we describe a new series of Ir(III) complexes consisting of chromophoric 2-(2-hydroxyphenyl)oxazole-based ancillary ligands. Interestingly, we observed direct optical excitation of the chromophoric ancillary ligand in these complexes, thus identifying two excitation species (both to the cyclometalating ligand and the chromophoric ancillary ligand) (Chart 1, case III). This double excitation potentially enables a favorable interligand energy harvesting process because phosphorescence of the Ir(III) complexes was generated from the chromophoric ancillary ligand only. Additionally, we sought to find a structure–property relationship in the phosphorescence of the resulting Ir(III) complexes by systematically modifying the 2-(2-hydroxyphenyl)oxazole ligand structure with an aim to establish the ligand design rule.

Scheme 1. Synthesis of the Chromophoric Ancillary Ligands

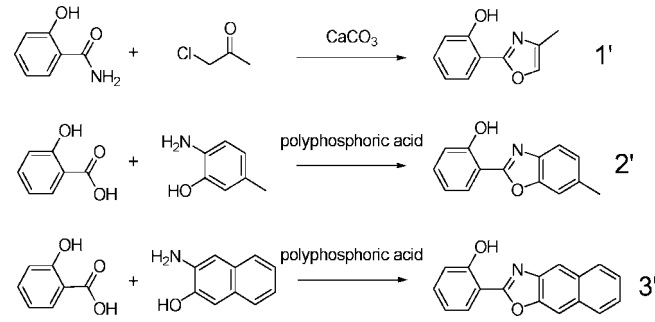

Three novel ancillary ligands (**1′**–**3′**; see Scheme 1 for their structures) structurally based on the 2-(2-hydroxyphenyl)oxazole unit were synthesized and subsequently incorporated into heteroleptic Ir(III) complexes. Their characteristic energy harvesting excitation and subsequent phosphorescence color tuning were comprehensively investigated using time-dependent density functional theory (TD-DFT) calculations, static and transient photoluminescence (PL) experiments, and cyclic voltammetry (CV) measurements. The color-tuned electrophosphorescence of these Ir(III) complexes was also demonstrated in OLEDs.

Experimental Section

Synthesis. Materials obtained from commercial suppliers were used without further purification unless otherwise stated. All glassware, syringes, magnetic stirring bars, and needles were thoroughly dried in a convection oven. Reactions were monitored using thin layer chromatography (TLC). Commercial TLC plates (silica gel 60 F_{254}, Merck Co.) were developed, and the spots were visualized under UV light at 254 and 365 nm, or stained with *p*-anisaldehyde. Silica gel column chromatography was performed with silica gel 60 G (particle size 5–40 μm, Merck Co.). 2-(2,4-Difluorophenyl)pyridine (dfppy) and μ-chloride-bridged Ir(III) dimer ($[(dfppy)_2Ir(\mu\text{-}Cl)]_2$) were synthesized according to the literature method.[3h]

2-(2-Hydroxyphenyl)-4-methyloxoazole (1′). A procedure in the literature[8b] was applied for this synthesis. ^{1}H NMR (300 MHz, $CDCl_3$) δ: 2.24 (s, 3H), 6.93 (t, J = 7.6 Hz, 1H), 7.06 (d, J = 8.3 Hz, 1H), 7.34 (t, J = 8.8 Hz, 1H), 7.40 (s, 1H), 7.80 (dd, J = 7.8 Hz, 1.6 Hz, 1H), 11.31 (s, 1H). ^{13}C NMR (75 MHz, $CDCl_3$) δ: 18.1, 112.4, 116.4, 122.3, 124.9, 129.4, 129.8, 137.7, 155.7, 160.9. MS (EI) *m*/*z* 175 (M^+), 146, 119, 106, 78. Anal. Calcd for $C_{10}H_9NO_2$: C, 68.56; H, 5.18; N, 8.00. Found: C, 68.71; H, 5.16; N, 7.95.

2-(2-Hydroxyphenyl)-6-methylbenzoxazole (2′). A procedure in the literature[8b] was applied for this synthesis. ^{1}H NMR (300 MHz, $CDCl_3$) δ: 2.52 (s, 3H), 7.00 (t, J = 7.6 Hz, 1H), 7.11 (d, J = 8.8 Hz, 1H), 7.20 (d, J = 8.1 Hz, 1H), 7.41 (m, 2H), 7.60 (d, J = 8.1 Hz, 1H), 8.01 (dd, J = 7.9 Hz, 1.7 Hz, 1H), 11.47 (s, 1H). ^{13}C NMR (75 MHz, $CDCl_3$) δ: 24.2, 119.0, 111.4, 116.4, 121.1, 121.4, 127.3, 128.4, 130.2, 133.1, 138.1, 148.4, 156.8, 162.7. MS (EI) *m*/*z* 225 (M^+), 197, 168, 147, 112, 98, 77. Anal. Calcd for $C_{14}H_{11}NO_2$: C, 74.65; H, 4.92; N, 6.22. Found: C, 74.71; H, 4.91; N, 6.21.

(4) (a) Nazeeruddin, M. K.; Humphry-Baker, R.; Berner, D.; Rivier, S.; Zuppiroli, L.; Graetzel, M. *J. Am. Chem. Soc.* **2003**, *125*, 8790–8797. (b) Tsuboyama, A.; Iwasaki, H.; Furugori, M.; Mukaide, T.; Kamatani, J.; Igawa, S.; Moriyama, T.; Miura, S.; Takiguchi, T.; Okada, S.; Hoshino, M.; Ueno, K. *J. Am. Chem. Soc.* **2003**, *125*, 12971–12979. (c) Lo, K. K.-M.; Chung, C.-K.; Lee, T. K.-M.; Lui, L.-H.; Tsang, K. H.-K.; Zhu, N. *Inorg. Chem.* **2003**, *42*, 6886–6897. (d) Tsuzuki, T.; Shirakawa, N.; Suzuki, T.; Tokito, S. *Adv. Mater.* **2003**, *15*, 1455–1458. (e) Baranoff, E.; Dixon, I. M.; Collin, J.-P.; Sauvage, J.-P.; Ventura, B.; Flamigni, L. *Inorg. Chem.* **2004**, *43*, 3057–3066. (f) Huang, W.-S.; Lin, J. T.; Chien, C.-H.; Tao, Y.-T.; Sun, A.-S.; Wen, Y.-S. *Chem. Mater.* **2004**, *16*, 2480–2488. (g) Yang, C.-H.; Tai C.-C.; Sun, I-W. *J. Mater. Chem.* **2004**, *14*, 947–950. (h) Anthopoulos, T. D.; Frampton, M. J.; Namdas, E. B.; Burn, P. L.; Samuel, I. D. W. *Adv. Mater.* **2004**, *16*, 557–560. (i) Sandee, A. J.; Williams, C. K.; Evans, N. R.; Davies, J. E.; Boothby, C. E.; Köhler, A.; Friend, R. H.; Holmes, A. B. *J. Am. Chem. Soc.* **2004**, *126*, 7041–7048. (j) Chen, X.; Liao, J.-L.; Liang, Y.; Ahmed, M. O.; Tseng, H.-E.; Chen, S.-A. *J. Am. Chem. Soc.* **2003**, *125*, 636–637. (k) Holder, E.; Langeveld, B. M. W.; Schubert, U. S. *Adv. Mater.* **2005**, *17*, 1109–1121. (l) Zhao, Q.; Liu, S.; Shi, M.; Wang, C.; Yu, M.; Li, L.; Li, F.; Yi, T.; Huang, C. *Inorg. Chem.* **2006**, *45*, 6152–6160. (m) Ragni, R.; Plummer, E. A.; Brunner, K.; Hofstraat, J. W.; Badudri, F.; Farinola, G. M.; Naso, F.; De Cola, L. *J. Mater. Chem.* **2006**, *16*, 1161–1170. (n) Huang, J.; Watanabe, T.; Ueno, K.; Yang, Y. *Adv. Mater.* **2007**, *19*, 739–743. (o) Wong, W.-Y.; Ho, C.-L.; Gao, Z.-Q.; Mi, B.-X.; Chen, C.-H.; Cheah, K.-W.; Lin, Z. *Angew. Chem., Int. Ed.* **2006**, *45*, 7800–7803. (p) Wong, W.-Y.; Zhou, G.-J.; Yu, X.-M.; Kwok, H.-S.; Tang, B.-Z. *Adv. Funct. Mater.* **2006**, *16*, 838–846. (q) King, S. M.; Al-Attar, H. A.; Evans, R. J.; Congreve, A.; Beeby, A.; Monkman, A. P. *Adv. Funct. Mater.* **2006**, *16*, 1043–1050. (r) Thomas, K. R. J.; Velusamy, M.; Lin, J. T.; Chien, C.-H.; Tao, Y.-T.; Wen, Y. S.; Hu, Y.-H.; Chou, P.-T. *Inorg. Chem.* **2005**, *44*, 5677–5685. (s) Yang, C. L.; Zhang, X. W.; You, H.; Zhu, L. Y.; Chen, L. Q.; Zhu, L. N.; Tao, Y. T.; Ma, D. G.; Shuai, Z. G.; Qin, J. G. *Adv. Funct. Mater.* **2007**, *17*, 651–661. (t) Yang, C.-H.; Cheng, Y.-M.; Chi, Y.; Hsu, C.-J.; Fang, F.-C.; Wong, K.-T.; Chou, P.-T.; Chang, C.-H.; Tsai, M.-H.; Wu, C.-C. *Angew. Chem., Int. Ed.* **2007**, *46*, 2418–2421.

(5) Wilde, A. P.; King, K. A.; Watts, R. J. *J. Phys. Chem.* **1991**, *95*, 629–634.

(6) (a) Coppo, P.; Plummer, E. A.; De Cola, L. *Chem. Commun.* **2004**, 1774–1775. (b) Yeh, S.-J.; Wu, M.-F.; Chen, C.-T.; Song, Y.-H.; Chi, Y.; Ho, M.-H.; Hsu, S.-F.; Chen, C. H. *Adv. Mater.* **2005**, *17*, 285–289. (c) Li, J.; Djurovich, P. I.; Alleyne, B. D.; Tsyba, I.; Ho, N. N.; Bau, R.; Thompson, M. E. *Polyhedron* **2004**, *23*, 419–428.

(7) (a) Kwon, T.-H.; Cho, H. S.; Kim, J.-W.; Kim, J.-J.; Lee, K. H.; Park, S. J.; Shin, I.-S.; Kim, H.; Shin, D. M.; Chung, Y. K.; Hong, J.-I. *Organometallics* **2005**, *24*, 1578–1585. (b) Kappaun, S.; Sax, S.; Eder, S.; Möller, K. C.; Waich, K.; Niedermaier, F.; Saf, R.; Mereiter, K.; Jacob, J.; Müllen, K.; List, E. J. W.; Slugovc, C. *Chem. Mater.* **2007**, *19*, 1209–1211. (c) You, Y.; Park, S. Y. *J. Am. Chem. Soc.* **2005**, *127*, 12438–12439. (d) You, Y.; Kim, K. S.; Ahn, T. K.; Kim, D.; Park, S. Y. *J. Phys. Chem. C* **2007**, *111*, 4052–4060.

(8) (a) For synthesis of **1′**: Guallar, V.; Moreno, M.; Lluch, J. M.; Amat-Guerri, F.; Douhal, A. *J. Phys. Chem.* **1996**, *100*, 19789–19794. (b) For synthesis of **2′** and **3′**: Nagaoka, S.; Kusunoki, J.; Fujibuchi, T.; Hatakenaka, S.; Mukai, K.; Nagashima, U. J. *Photochem. Phtobiol. A* **1999**, *122*, 151–159.

2-(2-Hydroxyphenyl)naphthoxazole (3′). A procedure in the literature[8b] was applied for this synthesis. ^{1}H NMR (300 MHz, $CDCl_3$) δ: 7.05 (td, J = 7.4 Hz, 1.1 Hz, 1H), 7.16 (dd, J = 8.4 Hz, 1.0 Hz, 1H), 7.52 (m, 2H), 7.99 (m, 3H), 8.10 (dd, J = 7.9 Hz, 1.6 Hz, 1H), 8.17 (s, 1H), 11.58 (s, 1H). ^{13}C NMR (75 MHz, $CDCl_3$) δ: 102.7, 115.4, 120.9, 121.1, 121.4, 122.6, 125.6, 127.3, 127.4, 127.6, 127.7, 128.9, 130.0, 141.7, 150.9, 154.3, 163.1. MS (EI) m/z 261 (M^+), 233, 204, 130, 114, 88. Anal. Calcd for $C_{17}H_{11}NO_2$: C, 78.15; H, 4.24; N, 5.36. Found: C, 78.09; H, 4.21; N, 5.34.

Iridium (III) bis(2-(2,4-difluorophenyl)pyridinato-*N*,*C*$^{2'}$) (2-(4-Methyloxazolyl)phenolate) (1). $[(dfppy)_2Ir(\mu\text{-}Cl)]_2$ (0.400 g, 0.330 mmol), sodium carbonate (0.349 g, 3.202 mmol), and **1′** (0.150 g, 0.855 mmol) were dissolved in 30 mL of 2-ethoxyethanol. After degassing, the reaction vessel was equilibrated with an Ar atmosphere. The temperature was then raised to 140 °C, and the reaction mixture was stirred for 5 h. The cooled crude mixture was poured into EtOAc (150 mL) and extracted with water (100 mL, three times) to remove 2-ethoxyethanol. Silica gel column purification with *n*-hexane:EtOAc (5:1, v/v) and reprecipitation in 50 mL of ether:*n*-hexane (1:4, v/v) gave a yellow powder (0.367 g, 75%). TLC, R_f = 0.2 (*n*-hexane:EtOAc = 5:1). ^{1}H NMR (500 MHz, $CDCl_3$) δ: 1.94 (s, 3H), 5.50 (dd, J = 8.7 Hz, 2.3 Hz, 1H), 5.82 (dd, J = 8.9 Hz, 2.3 Hz, 1H), 6.33–6.43 (br m, 3H), 6.62 (dd, J = 8.6 Hz, 0.9 Hz, 1H), 6.94 (t, 1H), 7.05–7.12 (br m, 2H), 7.68 (m, 2H), 7,77 (t, 1H), 8.09 (d, J = 5.9 Hz, 1H), 8.25 (t, J = 8.3 Hz, 2H), 8.94 (d, J = 5.8 Hz, 1H). ^{13}C NMR (125 MHz, $CDCl_3$) δ: 18.9, 105.2, 105.6, 112.4, 112.7, 112.8, 117.5, 120.9, 120.6. 121.8. 122.0, 122.1, 125.4, 125.7, 126.8, 129.5, 130.8, 131.3, 131.5, 137.0, 137.2, 138.4, 149.7, 150.0, 151.0, 155.6, 157.0, 157.3, 159.8, 160.0,,164.2, 165.0. DIP (direct injection probe) MS (FAB) m/z 747 (M^+ − 15), 573, 571, 307, 289, 154. Anal. Calcd for $C_{33}H_{23}F_4IrN_3O_2$: C, 52.03; H, 3.04; N, 5.52. Found: C, 51.96; H, 3.03; N, 5.35.

Iridium (III) bis(2-(2,4-difluorophenyl)pyridinato-*N*,*C*$^{2'}$) (2-(6-Methylbenzoxazolyl)phenolate) (2). The method used for **1**, but with **2′** (0.150 g, 0.666 mmol) instead of **1′**, was applied to give a yellow powder (0.388 g, 73%). TLC, R_f = 0.2 (*n*-hexane:EtOAc = 5:1). ^{1}H NMR δ: 2.39 (s, 3H), 5.60 (dd, J = 8.6 Hz, 2.3 Hz, 1H), 5.92 (dd, J = 8.8 Hz, 2.4 Hz, 1H), 6.42–6.54 (br m, 3H), 6.76 (t, J = 8.3 Hz, 2H), 6.91 (t, J = 6.0 Hz, 1H), 7.09 (t, J = 7.3 Hz, 1H), 7.20 (m, 2H), 7.72 (t, J = 8.3 Hz, 2H), 7.95 (dd, J = 8.2 Hz, 1.8 Hz, 1H), 8.10 (d, J = 5.8 Hz, 1H), 8.21 (d, J = 7.8 Hz, 1H), 8.30 (d, J = 8.5 Hz, 1H), 8.85 (d, J = 4.9 Hz, 1H). ^{13}C NMR (125 MHz, $CDCl_3$) δ: 24.8, 104.9, 105.2, 111.4, 111.9, 112.2, 116.4, 119.0, 120.1, 120.9, 120.9, 121.4, 122.0, 122.5, 123.1, 124.2, 126.7, 129.1, 129.5, 130.1, 130.8, 132.4, 137.1, 137.8, 138.0, 149.5, 149.5, 150.6, 153.3, 155.4, 156.4, 158.4, 160.0, 160.2, 163.0, 163.1. DIP MS (FAB) m/z 797 (M^+ − 15), 573, 571, 154. Anal. Calcd for $C_{37}H_{25}F_4IrN_3O_2$: C, 54.74; H, 3.10; N, 5.18. Found: C, 54.77; H, 3.10; N, 5.09.

Iridium (III) bis(2-(2,4-difluorophenyl)pyridinato-*N*,*C*$^{2'}$) (2-(Naphthoxazolyl)phenolate) (3). The method used for **1**, but with **3′** (0.223 g, 0.855 mmol) instead of **1′**, was applied to give a yellow powder (0.409 g, 73%). TLC, R_f = 0.2 (*n*-hexane:EtOAc = 4:1); ^{1}H NMR δ: 5.62 (dd, J = 8.6 Hz, 2.4 Hz, 1H), 6.00 (dd, J = 8.8 Hz, 2.3 Hz, 1H), 6.38–6.61 (br m, 4H), 6.77 (d, J = 8.7 Hz, 1H), 6.90 (t, J = 4.7 Hz, 1H), 7.09 (t, 1H), 7.40 (m, 3H), 7.81 (s, 1H), 7.83 (d, J = 9.4 Hz, 1H), 8.03 (dd, J = 8.3 Hz, 1.8 Hz, 1H), 8.29 (m, 2H), 8.82 (d, J = 6.0 Hz, 1H), 8.87 (d, J = 4.8 Hz, 1H). ^{13}C NMR (125 MHz, $CDCl_3$) δ: 101.7, 105.2, 105.7, 111.8, 111.8, 116.5, 120.3, 120.7, 121.1, 121.3, 121.4, 121.9, 122.4, 123.9, 124.1, 124.3, 125.1, 127.5, 127.9, 128.0, 128.1, 128.2, 128.4, 130.1, 130.1, 136.4, 138.4, 139.5, 148.5, 149.7, 151.2, 152.2, 156.4, 157.6, 157.6, 158.6, 159.1, 163.5, 163.5. DIP MS (FAB) m/z 833 (M^+), 643, 573, 553, 154. Anal. Calcd for $C_{40}H_{25}F_4IrN_3O_2$: C, 56.66; H, 2.97; N, 4.96. Found: C, 56.87; H, 3.24; N, 4.69.

Characterization. Absorption spectra of the complexes in solution or in doped poly(methylmethacrylate) (PMMA) films were recorded with Shimazu UV-1650PC from 280 to 700 nm. The films were prepared by spin-coating a solution of PMMA and the complex in 1,2-dichloroethane (5 wt %) on precleaned glass substrates at 2000 rpm. Photoluminescence spectra were obtained with a Shimazu RF 5301 PC spectrophotometer in the range of 400–700 nm. Absorption and PL spectra of Ir(III) complex solutions were measured after Ar-saturation. CV experiments were carried out with a model 273A instrument (Princeton Applied Research) using three electrode cell assemblies. Measurements were carried out in dichloromethane solution with tetrabutylammonium tetrafluoroborate as a supporting electrolyte at a scan rate of 100 mV/s. Each oxidation potential was calibrated with that of ferrocene.

Quantum chemical calculations based on DFT were carried out using the Dmol^3 module installed in Materials Studio (Accelrys Inc.).[9] Ground-state geometry optimization and single point calculations were performed using a blyp functional and a DNP basis set under an effective core potential. SCF tolerance was maintained within 10^{-6}. For the TD-DFT calculations, Gaussian03 software (Gaussian Inc.) was used.[10] On the basis of the optimized ground-state geometry, a "double-ζ" quality basis set of lanl2dz for the Ir atom and 6-31g** for the other atoms were applied together with the b3lyp functional. Typically, the lowest 5 triplet and 5 singlet states were obtained.

For the time-resolved PL measurements, an excitation pulse of 355 nm was generated from the third harmonic output of a Q-switched Nd:YAG laser (Continuum, Surelite), and an excitation pulse of 480 nm was generated from OPO laser (Continium, Surelite-OPO). The pulse width was 6 ns. However, the temporal resolution of the PL data was less than a third of this pulse duration by using a least-squares deconvolution fitting process (LIFETIME program with an iterative nonlinear-square deconvolution procedure developed at the University of Pennsylvania). The emission light was collimated before entering the monochromator slit and then spectrally resolved using a 15 cm monochromator (Acton Research, SP150) equipped with a 600 grooves/mm grating after passing the sample. The light signal was detected via a photomultiplier tube (Hamamatsu, R928). The output signal from the photomultiplier tube was recorded with a 500 MHz digital storage oscilloscope (Tektronix, TDS3052) for the temporal profile measurement.

Device Fabrication. A patterned indium tin oxide (ITO) coated glass substrate with a sheet resistance of 15 Ω/square was used for

(9) (a) Delley, B. *J. Chem. Phys.* **1990**, *92*, 508–517. (b) Delley, B. *J. Chem. Phys.* **2000**, *113*, 7756–7764; DMol^3 is available as part of Materials Studio.

(10) Frisch, M. J.; Trucks, G. W.; Schlegel, H. B.; Scuseria, G. E.; Robb, M. A.; Cheeseman, J. R.; Montgomery, J. A., Jr.; Vreven, T.; Kudin, K. N.; Burant, J. C.; Millam, J. M.; Iyengar, S. S.; Tomasi, J.; Barone, V.; Mennucci, B.; Cossi, M.; Scalmani, G.; Rega, N.; Petersson, G. A.; Nakatsuji, H.; Hada, M.; Ehara, M.; Toyota, K.; Fukuda, R.; Hasegawa, J.; Ishida, M.; Nakajima, T.; Honda, Y.; Kitao, O.; Nakai, H.; Klene, M.; Li, X.; Knox, J. E.; Hratchian, H. P.; Cross, J. B.; Bakken, V.; Adamo, C.; Jaramillo, J.; Gomperts, R.; Stratmann, R. E.; Yazyev, O.; Austin, A. J.; Cammi, R.; Pomelli, C.; Ochterski, J. W.; Ayala, P. Y.; Morokuma, K.; Voth, G. A.; Salvador, P.; Dannenberg, J. J.; Zakrzewski, V. G.; Dapprich, S.; Daniels, A. D.; Strain, M. C.; Farkas, O.; Malick, D. K.; Rabuck, A. D.; Raghavachari, K.; Foresman, J. B.; Ortiz, J. V.; Cui, Q.; Baboul, A. G.; Clifford, S.; Cioslowski, J.; Stefanov, B. B.; Liu, G.; Liashenko, A.; Piskorz, P.; Komaromi, I.; Martin, R. L.; Fox, D. J.; Keith, T.; Al-Laham, M. A.; Peng, C. Y.; Nanayakkara, A.; Challacombe, M.; Gill, P. M. W.; Johnson, B.; Chen, W.; Wong, M. W.; Gonzalez, C.; Pople, J. A. *Gaussian 03*, rev C.02; Gaussian, Inc.: Wallingford, CT, 2004.

Scheme 2. Synthesis of **1**, **2**, **3**, and a Comparative Ir(III) Complex, FIrpic Ir(III) bis(2-(2,4-Difluorophenyl)pyridinato-*N*,$C^{2'}$) picolinate)

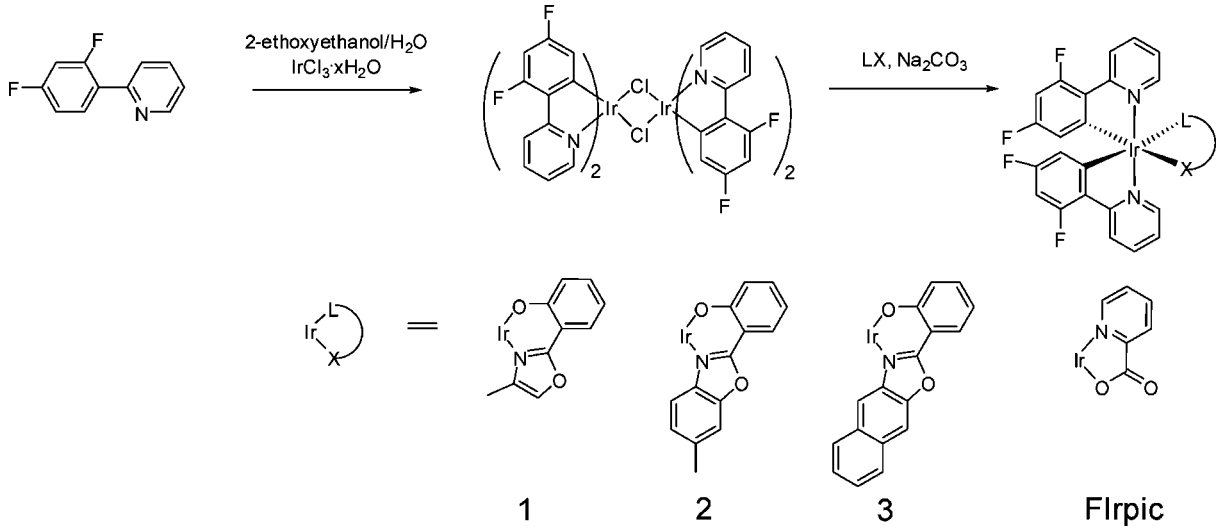

the anode of each OLED. The ITO-coated glass substrate was precleaned with boiling ethanol and deionized water and then treated in an O_2-plasma chamber before loading into an organic evaporation chamber. A hole-injecting copper(II) phthalocyanine (CuPc) layer and a hole-transporting 4,4′-bis[*N*-(1-naphthyl)-*N*-phenylamino]biphenyl (NPD) layer were then sequentially deposited, after which a 30-nm-thick layer comprised of the Ir(III) complex and 4,4′-*N*,*N*′-dicarbazolebiphenyl (CBP) was deposited by coevaporation. Then, a hole-blocking aluminum(III) bis(2-methyl-8-quinolinate)(4-phenylphenolate) (BAlq) layer and an electron-transporting aluminum(III) tris(8-quinolinate) (Alq_3) layer were deposited. Finally, a LiF and aluminum metal cathode was deposited by thermal evaporation. Thus, the OLED device configuration was ITO/CuPc(10 nm)/NPD(40 nm)/Ir:CBP(30 nm)/BAlq(10 nm)/Alq_3(30 nm)/LiF:Al(150 nm). All deposition processes were performed under a base pressure of 5×10^{-6} Torr without breaking the vacuum between the different deposition processes. The emissive area of the device, as defined by the overlapping rectangular area of the cathode and anode, was 2×2 mm^2. Current–voltage−luminance characteristics of the devices were obtained using a Keithley 237 source measure unit connected to CA-100A luminance meter (Minolta). Electroluminescence (EL) spectra were recorded with an Ocean Optics USB2000 fiber optic spectrometer.

Results and Discussion

In most Ir(III) complexes containing 2-phenylpyridine (ppy)-type cyclometalating ligands, the highest occupied molecular orbital (HOMO) is spread over the Ir and the anionic phenyl ring, whereas the lowest unoccupied molecular orbital (LUMO) is mostly localized on the neutral pyridine ring of the cyclometalating ligand.[3j,5,11] Considering the configuration of OLEDs, proper energy level matching between the host material and the Ir(III) complex is an important issue because a higher device efficiency is ensured only when the oxidation potential (HOMO energy) and the excited-state energy of the Ir(III) complex are located within those of the host material.[12] For the phosphorescence color tuning, HOMO tuning is not recommended for OLED applications because the oxidation potentials of most Ir(III) complexes are already very close to those of generally used arylamine-type hosts such as CBP. Instead, tuning of the excited-state energy by altering the LUMO is recognized as a more effective approach. Hence, it is reasonable to control the LUMO energy of the chromophoric ancillary ligands for phosphorescence color tuning of their Ir(III) complexes. For the present Ir(III) complexes incorporating 2-(2-hydroxyphenyl)oxazole ligands, DFT calculations predict that the anionic phenolate ring of the ligand contributes to the HOMO while the neutral oxazole unit contributes to the LUMO (see below). Additionally, DFT calculation results indicated that the LUMO energy of the ancillary ligand was lowered with increasing number of phenyl rings fused to the oxazole unit, whereas the HOMO level showed relatively small change. Therefore, a progressive bathochromic shift of phosphorescence is predicted with going from complex **1** to **3** in the present series of Ir(III) complexes (see Scheme 2 for the structures).

Substituting the ancillary ligands for the chlorides of the μ-chloride-bridged Ir(III) dimer ($(C^N)_2Ir(\mu\text{-}Cl)_2Ir(C^N)_2$) to give cyclometalated heteroleptic Ir(III) complexes proceeded in good yield, and the products were easily purified by silica gel column chromatography. Because the 2-(2-hydroxyphenyl)oxazole ligands have been extensively investigated for their excited-state intramolecular proton transfer (ESIPT) characteristics, diverse syntheses have been established potentially enabling us to prepare a range of homologous Ir(III) complexes (**1**–**3**).[8,13] The Ir(III) complexes **1**–**3** all

(11) (a) Colombo, M. G.; Guedel, H. U. *Inorg. Chem.* **1933**, *32*, 3081–3087. (b) Hwang, F.-M.; Chen, H.-Y.; Chen, P.-S.; Liu, C.-S.; Chi, Y.; Shu, C.-F.; Wu, F.-I.; Chou, P.-T.; Peng, S.-M.; Lee, G.-H. *Inorg. Chem.* **2005**, *44*, 1344–1353.

(12) (a) Ren, X.; Li, J.; Holmes, R. J.; Djurovich, P. I.; Forrest, S. R.; Thompson, M. E. *Chem. Mater.* **2004**, *16*, 4743–4747. (b) Tokito, S.; Iijima, T.; Suzuri, Y.; Kita, H.; Tsuzuki, Y.; Sato, F. *Appl. Phys. Lett.* **2003**, *83*, 569–571.

(13) (a) Roberts, E. L.; Chou, P. T.; Alexander, T. A.; Agbaria, R. A.; Warner, I. M. J. *Phys. Chem.* **1995**, *99*, 5431–5437. (b) Chou, P.-T.; Huang, C.-H.; Pu, S.-C.; Cheng, Y.-M.; Liu, Y.-H.; Wang, Y.; Chen, C.-T. *J. Phys. Chem. A* **2004**, *108*, 6452–6454. (c) Yu, W.-S.; Cheng, C.-C.; Cheng, Y.-M.; Wu, P.-C.; Song, Y.-H.; Chi, Y.; Chou, P.-T. *J. Am. Chem. Soc.* **2003**, *125*, 10800–10801.

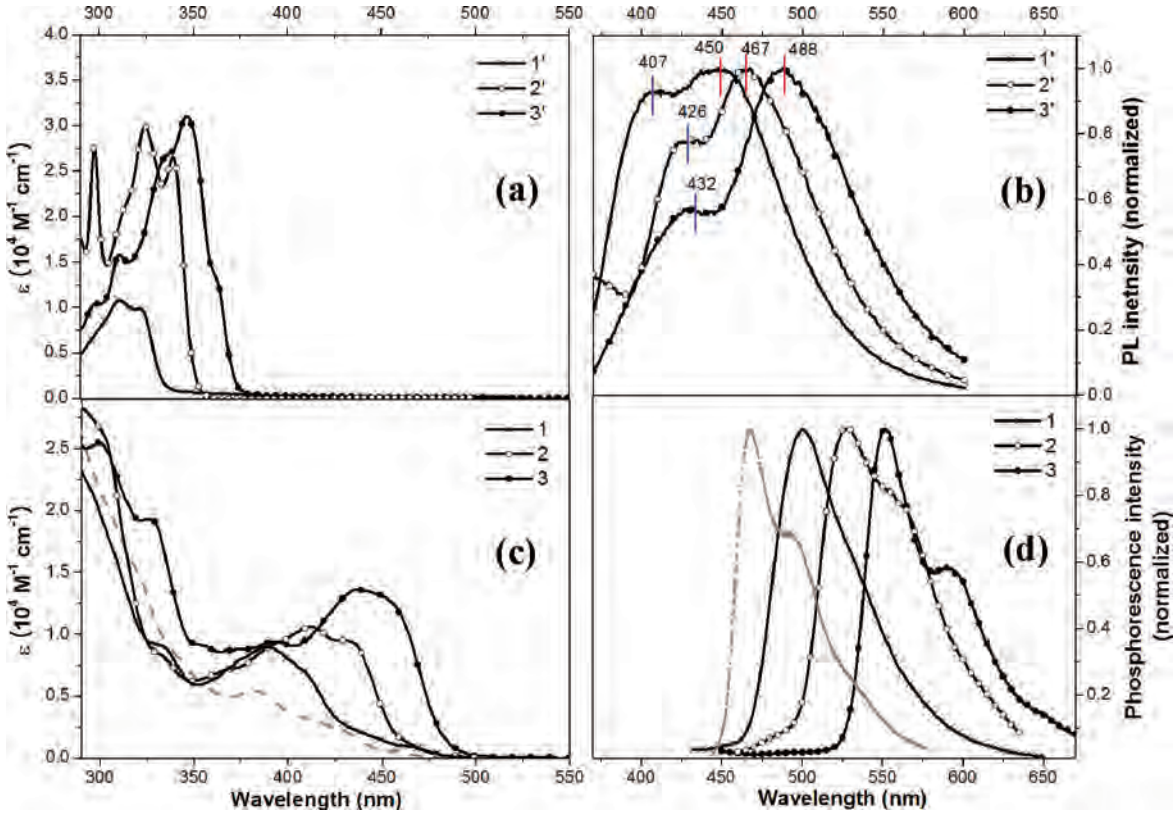

Figure 1. Absorption (a) and photoluminescence (b) spectra of the ligands used in the Ir(III) complexes (**1′**−**3′**, THF:MeOH 1/9, v/v, 1.0×10^{-5} M). Blue and red marks in the spectra of part b indicate peak positions of enol and keto emissions, respectively. See text for the explanation. Absorption (c) and phosphorescence (d) spectra of the Ir(III) complexes (**1**–**3**, toluene, 1.0×10^{-5} M). The grey lines show the absorption and phosphorescence spectra of the Ir(III) complex (iridium(III) bis[(4,6-difluorophenyl)-pyridinato-*N,C*$^{2'}$]picolinate, FIrpic) which exhibits cyclometalating ligand (same cyclometalating ligand as in **1**−**3**) centered phosphorescence.

exhibited fairly good solubility in common organic solvents such as dichloromethane, toluene, acetonitrile, and acetone. Also, during long-term storage in *N,N*-dimethylforamide, methylsulfoxide, acetone, or acetonitrile, the complexes did not undergo solvent-induced decomposition even after 3 months, as shown by ^{1}H NMR spectroscopy.

In the absorption spectra of complexes **1**–**3** (Figure 1c), strong (log $\varepsilon \sim 4$) and structured absorption peaks (around 350–420 nm for **1**, 370–450 nm for **2**, and 400–500 nm for **3**) are observed in a lower energy region than that of the singlet cyclometalating ligand centered (^1L_CC) transition (<350 nm), and they exhibit significant overlap between the metal to cyclometalating ligand charge-transfer (ML_CCT) transition bands (>380 nm).[5] As clearly shown, this absorption band tends to move to lower energy as the bandgap of the ancillary ligand is decreased (i.e., on going from **1** to **3**). This spectral trend is different from those of the previously reported heteroleptic Ir(III) complexes with pyridylcarboxylate chromophoric ancillary ligands.[7c,d] Compared to the absorption spectra of their respective free ligands (**1′**, **2′**, and **3′**; see Figure 1a), molar absorbance of these new bands are almost $^1/_3$ of those of free ligands. In addition, the shapes of the vibronic peaks in the spectra of the complexes strongly resemble those of the free ancillary ligands, suggesting that, in this case, direct excitation to the ancillary ligands is involved. Thus, we can infer that the ancillary ligands (**1′**−**3′**) are related to the optical excitation responsible for this absorption behavior. From the absorption spectra, it is found that this direct excitation of the chromophoric ancillary ligand needs higher energy than that required for the triplet transition of the cyclometalating ligand for **1** but has similar energy for **2** and lower energy for **3**. Furthermore, because the excitation spectra of the Ir(III) complexes also have intense peaks in the ^1L_CC transition region (<350 nm; see the Supporting Information), it is considered that the excitation occurred at both ligands (the cyclometalating ligand and the ancillary ligand) simultaneously. The strong dual absorptions of the present Ir(III) complexes—the ancillary ligand centered absorption as well as the cyclometalating ligand centered absorption—allow the complexes to strongly absorb light over a broader spectral range, which is a favorable characteristic for potential use of the complexes in the solar cell, biological labeling agent, and photooxidant applications.[14] Likewise, efficient Förster energy transfer from a host to the Ir(III) complexes might be facilitated, which would enhance the efficiency of the complexes in OLED applications.[15]

All of the synthesized Ir(III) complexes were highly phosphorescent. They exhibited emission lifetimes ranging from 1.65 to 9.88 μs, which are suitable for OLED

(14) (a) Lo, K. K. W.; Ng, D. C. M.; Chung, C. K. *Organometallics* **2001**, *20*, 4999–5001. (b) Demas, J. N.; Harris, E. W.; McBride, R. P. *J. Am. Chem. Soc.* **1977**, *99*, 3547–3551. (c) Gao, R.; Ho, D. G.; Hernandez, B.; Selke, M.; Murphy, D.; Djurovich, P. I.; Thompson, M. E. *J. Am. Chem. Soc.* **2002**, *124*, 14828–14829.

(15) Baldo, M. A.; Adachi, C.; Forrest, S. R. *Phys. Rev. B* **2000**, *62*, 10967–10977.

Table 1. Photophysical and Electrochemical Properties of the Ir(III) Complexes **1**–**3**

complex	absorbance λ_{max} (nm) (log ε)[a]	emission λ_{max} (nm) solution[a]	emission λ_{max} (nm) film[b]	IP (eV)[c]	Φ[d]	τ_{ems} (μs)	k_r ($\times 10^5$ s^{-1})	k_{nr} ($\times 10^5$ s^{-1})	τ_{ILET} (ns)
1	405 (3.87), 389 (3.95), 332 (5.96), 285 (4.38)	500	502	5.44	0.36	1.65	2.18	3.88	3.9 ± 0.4
2	432 (3.98), 412 (4.02), 332 (3.92), 295 (4.44)	525	524	5.52	0.41	7.25	0.57	1.39	5.5 ± 0.5
3	438 (4.13), 391 (3.97), 373 (3.94), 326 (4.29)	552	548	5.55	0.43	9.88	0.44	0.58	3.4 ± 0.1

[a] 1.0×10^{-5} M in Ar-saturated toluene. [b] Poly(methylmethacrylate) films doped with 5 wt % of the Ir(III) complex. [c] Ionization (oxidation) potential measured by CV (condition: Pt wires as the working and counter electrodes; 0.1 M tetrabutylammonium tetrafluoroborate as the supporting electrolyte in dichloromethane solution; Ag wire as the pseudo-reference electrode; ferrocene was used as the external reference.); The following equation is used to adjust the value relative to vacuum level: IP (eV) = E_{ox}(Ir) − E_{ox}(ferrocene) + 4.8. [d] Measured in Ar-saturated toluene solution (1.0×10^{-5} M) at room temperature. fac-Ir(ppy)$_3$ (0.40) was used as a standard material.

Chart 2. Change in the Phosphorescence Energy with Increasing Number of Fused Phenyl Rings

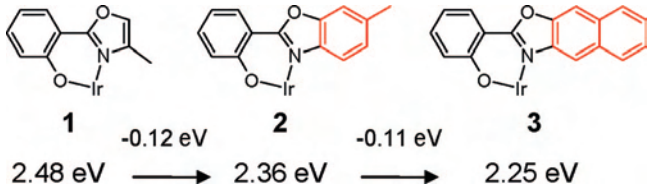

applications.[16] Moreover, the phosphorescence quantum efficiencies of **1**–**3** were measured to be 0.36, 0.41, and 0.43, respectively, which are as high as that of the most typical Ir(III) complex, Ir(ppy)$_3$ (0.40).[17] As summarized in Table 1, the phosphorescence color is bathochromically shifted in a stepwise manner from greenish blue (500 nm, **1**) to yellow (552 nm, **3**), indicating that the color can be effectively tuned by varying the number of phenyl rings fused to the oxazole unit in the ancillary ligand. This bathochromic shift is initially expected from the fluorescence of the free ancillary ligands as shown in Figure 1b: although their fluorescence spectra exhibit rather broad dual emission originated from both enol- and keto-emissions even in a protic solvent (THF/MeOH), a bathchromic trend is clearly observed.[18] In addition, we found that the sequential fusion of phenyl rings to the oxazole unit induced a quite regular red-shift in the phosphorescence, by 52 nm (0.23 eV) for **3** and 25 nm (0.12 eV) for **2** with respect to that of **1**; thus, each fused phenyl ring induces a red shift of ca. 0.11 eV in the phosphorescence spectrum (Chart 2). Given the general lack of understanding of the correlation between the triplet-state energy and molecular structure of ligands for Ir(III) complexes, this regular and systematic control is quite interesting as a mean of further manipulating the triplet-state energy.

As shown in Table 1, the oxidation potential of the synthesized Ir(III) complexes gradually increases in small increments (<0.11 eV) as the number of phenyl rings fused to the oxazole unit is increased. Considering that the change in energy of the phosphorescence spectra (**1**−**3**) is 0.24 eV, this HOMO alteration is believed to have a minor effect on the phosphorescence color. According to the DFT calculations (see Figure 2), the HOMOs of all of the complexes are mainly localized over either the Ir atom or the phenolate ring of the ancillary ligand. This accounts for why the HOMO (oxidation potential) level is less affected by the variations in the ancillary ligand structure in the series of complexes, because our tuning modifications are restricted to the oxazole ring.

It is well-known that a charge-transfer emission such as MLCT phosphorescence is characterized by a broad and unstructured photoluminescence spectrum.[3j,19,20] For the photoluminescence spectra of **3** (Figure 1d), the apparent vibronic structure (1171 cm^{-1}) is observed which possibly correspond to rich contribution of LC transitions for the phosphorescence. Additional evidence implying an LC-rich transition was obtained by comparing the phosphorescence spectra of the complexes in solution (1.0×10^{-5} M, toluene) and in doped films (5 wt % doped, PMMA; Supporting Information). Generally, the degree of charge redistribution during an optical transition is qualitatively estimated by the characteristic rigidochromism, as dipolar relaxation of the charge-transfer transition states is largely controlled by the viscosity of the matrix.[3i,4b,19] Normally, a blue-shift is observed for a charge-transfer emission in a more rigid matrix, whose behavior results from a perturbed dipolar relaxation of the charge-transfer transition state. For example, characteristic rigidochromism has been observed in the heteroleptic Ir(III) complex with pyridylcarboxylate chromophoric ancillary ligands;[7d] in that case, the major transition responsible for the phosphorescence was the MLCT state whose energy was transferred to the ancillary ligand-mediated state in which considerable intramolecular charge-transfer (ICT) character was involved (Chart 1 case II). For the present Ir(III) complexes with chromophoric 2-(2-hydroxyphenyl)oxazole ancillary ligands, no rigidochromism was observed; that is, we found virtually no shift in the peak wavelength of the phosphorescence spectra on going from the solution to the film state, as summarized in Table 1. Finally, we could find that the energy of the phosphorescence peak maximum of the Ir(III) complexes was invariant with the changing polarity of solvents (see the Supporting Information). The present findings indicate that charge-transfer transitions are not significantly involved in our major emission pathway, leading us to presume that the most probable state for phosphorescence is the chromophoric

(16) Compared to the phosphorescence lifetime (0.2–2.5 s) of our previous Ir(III) complexes exhibiting interligand energy transfer (ILET) but lacking direct excitation of the chromophoric ancillary ligands, these phosphorescence lifetimes of **1**–**3** are not significantly changed.

(17) Sprouse, S.; King, K. A.; Spellane, P. J.; Watts, R. J. *J. Am. Chem. Soc.* **1984**, *106*, 6647–6653.

(18) Chang, D. W.; Kim, S.; Park, S. Y.; Yu, H.; Jang, D.-J. *Macromolecules* **2000**, *33*, 7223–7225.

(19) (a) Colombo, M. G.; Hauser, A.; Guedel, H. U. *Inorg. Chem.* **1993**, *32*, 3088–3092. (b) Flamigni, L.; Ventura, B.; Barigelletti, F.; Baranoff, E.; Collin, J.-P.; Sauvage, J.-P. *Eur. J. Inorg. Chem.* **2005**, 1312–1318.

(20) (a) Islam, A.; Ikeda, N.; Nozaki, K.; Ohno, T. J. *Photochem. Phtobiol. A* **1997**, *106*, 61–66. (b) Gabrielsson, A.; Zalis, S.; Matousek, P.; Towrie, M.; Vlcek, A., Jr *Inorg. Chem.* **2004**, *43*, 7380–7388. (c) Collman, J. P.; Barnes, C. E.; Swepston, P. N.; Ibers, J. A. *J. Am. Chem. Soc.* **1984**, *106*, 3500–3510.

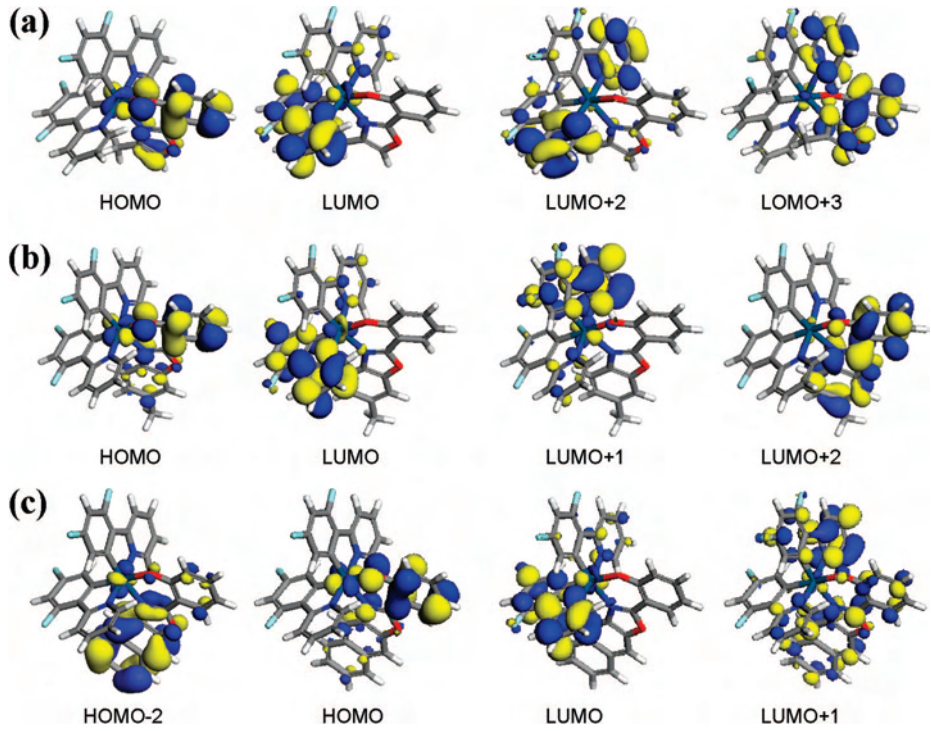

Figure 2. Important molecular orbitals of (a) **1**, (b) **2**, and (c) **3**.

ancillary ligand centered state (L_AC) which exhibits weak interaction with a charge-transfer state (e.g., MLCT).

In contrast, the relatively broad spectral shape of phosphorescence of **1** and change in the phosphorescence lifetime among **1**−**3** indicate that the degree of charge-transfer character increases from **3** to **1**: we could find a previous report that increased the charge-transfer character results in a decreased phosphorescence lifetime and broad spectral shape of phosphorescence.[11a,21] This trend is clearly observed on going from **3** to **1**. In addition, referring to previous comments that exchange energy ($\Delta E_{\text{singlet–triplet}}$) of a LC transition state is generally larger than that of a MLCT transition state,[3j] we may conclude that the ^3L_AC state is a dominant state for phosphorescence but the degree of interaction between a charge-transfer transition state increases from **3** to **1**. This explanation can be further supported from our TD-DFT calculation results which show that the lowest triplet state has L_AC character but takes substantial amount of mixing with a charge-transfer transition state (ML_CCT, L_AL_CCT, or ML_ACT).

In the study of transition metal complexes, quantum chemical calculations based on TD-DFT provide clear and qualitative implications when considering electronic transitions related to the photoluminescence.[4t,22] We performed TD-DFT (b3lyp/6-31g**:lanl2dz) calculations to investigate the excited states of **1** to **3**. As summarized in Table 2, we found quite good correlation between the calculated lowest triplet state energy and the measured phosphorescence energy for each Ir(III) complex (Table 1). One of our more important findings is that, although the HOMO → LUMO transition exclusively gives the lowest singlet excited state (S_1, except **3**), the lowest triplet state (T_1) is largely associated with the HOMO → higher-lying LUMO transitions. For example, the HOMO → LUMO + 2 transition leads to the T_1 of **2**, both the HOMO → LUMO + 2 and HOMO → LUMO + 3 transitions largely contribute to the T_1 of **1**, and HOMO → LUMO + 1 contributes to the T_1 of **3**. These results explain to the ancillary ligand-enriched character of the resulting triplet states because the higher-lying LUMOs are localized over the chromophoric ancillary ligands. As shown in Figure 2, although the LUMO is located over the cyclometalating ligand, the higher-lying LUMOs (LUMO + 3 for **1**; LUMO + 2 for **2**; and LUMO + 1 for **3**), which determine the T_1 state, are dominated by the ancillary ligands. Hence, we can say that the lowest spin-allowed transition is composed of excitation processes involving the LUMO of the cyclometalating ligand (i.e., ML_CCT, L_AL_CCT, and L_CC in Table 2). On the contrary, the triplet transition is afforded by the LUMO of the ancillary ligand (i.e., L_AC in Table 2). However, as the phosphorescence process mainly involves the triplet transition, ancillary-ligand-mediated phosphorescence is expected. This finding is consistent with the observed absorption and phosphorescence behaviors of **1**−**3**, revealing the single chromophoric ancillary ligand-centered phosphorescence and double excitations to both the cyclometalating ligand and the ancillary ligand (Chart 1, case III).

(21) Wilkinson, A. J.; Puschmann, H.; Howard, J. A. K.; Foster, C. E.; Williams, J. A. G. *Inorg. Chem.* **2006**, *45*, 8685–8699.

(22) (a) Hay, P. J. *J. Phys. Chem. A* **2002**, *106*, 1634–1641. (b) Avilov, I.; Minoofar, P.; Cornil, J.; De Cola, L. *J. Am. Chem. Soc.* **2007**, *129*, 8247–8258. (c) Liu, T.; Xia, B.-H.; Zhou, X.; Zhang, H.-X.; Pan Q.-J.; Gao, J.-S. *Organometallics* **2007**, *26*, 143–149. (d) Yeh, Y.-S.; Cheng, Y.-M.; Chou, P.-T.; Lee, G.-H.; Yang, C.-H.; Chi, Y.; Shu, C.-F.; Wang, C.-H. *ChemPhysChem* **2006**, *7*, 2294–2297.

Table 2. TD-DFT Calculation Results of the Ir(III) Complexes

state	transition energy	participating MO	transition character[a]
		1	
T_1	503.4 nm	HOMO → LUMO (0.25)[b]	$L_AC + L_AL_CCT + ML_CCT$
		HOMO → LUMO + 2 (0.59)	
		HOMO → LUMO + 3 (0.31)	
T_2	489.3 nm	HOMO → LUMO (0.57)	$L_AL_CCT + ML_CCT$
		HOMO → LUMO + 1 (0.29)	
		HOMO → LUMO + 2 (0.25)	
S_1	483.9 nm ($f = 0.0025$)[c]	HOMO → LUMO (0.70)	$L_AL_CCT + ML_CCT$
		2	
T_1	533.4 nm	HOMO → LUMO + 2 (0.75)	$L_AC + ML_ACT$
T_2	478.4 nm	HOMO → LUMO (0.56)	$L_AL_CCT + ML_CCT$
		HOMO → LUMO + 1 (0.38)	
S_1	470.8 nm ($f = 0.0010$)	HOMO → LUMO (0.70)	$L_AL_CCT + ML_CCT$
		3	
T_1	575.4 nm	HOMO → LUMO (0.66)	$L_AC + ML_ACT + ML_CCT + L_AL_CCT$
		HOMO → LUMO + 1 (0.22)	
T_2	494.0 nm	HOMO − 2 → LUMO (0.62)	$ML_CCT + L_AL_CCT + L_AC$
		HOMO − 2 → LUMO + 3 (0.24)	
T_3	467.9 nm	HOMO → LUMO + 1 (0.45)	$L_AC + ML_ACT + ML_CCT + L_AL_CCT$
		HOMO → LUMO + 2 (0.44)	
S_1	461.4 nm ($f = 0.0038$)	HOMO → LUMO (0.30)	$L_AC + ML_ACT + ML_CCT + L_AL_CCT$
		HOMO → LUMO + 1 (0.63)	

[a] Used terminology: L_AC (the ancillary ligand-centered transition, i.e. ancillary ligand MO → ancillary ligand MO), L_AL_CCT (the ancillary ligand to the cyclometalating ligand charge-transfer transition, i.e. ancillary ligand MO → cyclometalating ligand MO), ML_CCT (Ir metal to the cyclometalating ligand transition, i.e. Ir d-orbital → cyclometalating ligand MO), ML_ACT (Ir metal to the ancillary ligand transition, i.e. Ir d-orbital → ancillary ligand MO). [b] Expansion coefficient. [c] Oscillator strength.

Our unique photophysical mechanism of dual excitation leading to a single phosphorescence emission requires an excited-state energy transfer process from the initially excited cyclometalating ligand state to the lower energy ancillary ligand state (i.e., interligand energy transfer [ILET]). We successfully monitored this ILET process by analyzing the transient photoluminescence of the Ir(III) complexes as shown in Figure 3. When each Ir(III) complex was excited at 355 nm where the cyclometalating ligands absorb, the cyclometalating ligand mediated phosphorescence was observed initially but disappeared within a few nanoseconds. In the same period, the ancillary ligand mediated phosphorescence emerged and was sustained for several microseconds. In contrast, direct excitation of the chromophoric ancillary ligand of **3** at 480 nm gave a prompt appearance of the ancillary ligand phosphorescence without having this early time rise of the ancillary ligand phosphorescence (see the Supporting Information). Hence, this time scale can be understood to be the ILET time (τ_{ILET}); the τ_{ILET} data for **1**−**3** are summarized in Table 1. Because the cyclometalating ligand mediated phosphorescence inherently exhibits a phosphorescence lifetime of 1.4 μs in solution,[23] the observed decrease in this phosphorescence lifetime of the cyclometalating ligand to several nanoseconds unambiguously indicates the existence of an additional decay channel in the excited state (Figure 4). This additional decay channel can be confidently assigned to energy transfer to the neighboring low energy ancillary ligand, which has been comprehensively examined in our previous work.[7d] This observation enables us to calculate the ILET efficiency using the following equation:[24]

$$\Phi_{ILET} = 1 - \frac{\tau_c}{\tau_{ca}} \quad (1)$$

where Φ_{ILET} represents the ILET efficiency, and τ_{ca} and τ_c denote the phosphorescence lifetimes of the cyclometalating ligand without and with ILET, respectively. Using $\tau_{ca} = 1.4$ μs and $\tau_c = 4.3$ (**1**), 5.0 (**2**), and 3.4 ns (**3**), we find using eq 1 that Φ_{ILET} values exceed 99% for all three complexes (**1** 99.7%, **2** 99.6%, and **3** 99.8%). Therefore, the excited-state energy of the cyclometalating ligand is exclusively transferred to the chromophoric ancillary ligand where phosphorescence is generated.

Although the Φ_{ILET} values of our Ir(III) complexes are high enough to guarantee effective energy transfer, the observed time scale of ILET (see Table 1) is noted to be longer than a previously reported interligand or intraligand energy transfer time scale of Ru(II) complexes which is generally on the several picoseconds or sub-picoseconds scale.[25] For example, Benniston et al. observed sub-picosecond intramolecular energy transfer from the ^{3}MLCT state of a terpyridine ligand to a $^3(\pi-\pi^*)$ state of a conjugatively linked free-base porphyrin.[25a] In addition,

(23) The transient PL of FIrpic was measured using the same experimental configuration.

(24) (a) Justin Thomas, K. R.; Thompson, A. L.; Sivakumar, A. V.; Bardeen, C. J.; Thayumanavan, S. *J. Am. Chem. Soc.* **2005**, *127*, 373–383. (b) Palilis, L. C.; Melinger, J. S.; Wolak, M. A.; Kafafi, Z. H. *J. Phys. Chem. B* **2005**, *109*, 5456–5463. (c) Shi, M.; Li, F.; Yi, T.; Zhang, D.; Hu, H.; Huang, C. *Inorg. Chem.* **2005**, *44*, 8929–8936.

(25) (a) Benniston, A. C.; Chapman, G. M.; Harriman, A.; Mehrabi, M. *J. Phys. Chem. A* **2004**, *108*, 9026–9036. (b) Faiz, J. A.; Williams, R. M.; Silva, M. J. J. P.; De Cola, L.; Pikramenou, Z. *J. Am. Chem. Soc.* **2006**, *128*, 4520–4521. (c) Harriman, A.; Romero, F. M.; Ziessel, R.; Benniston, A. C. *J. Phys. Chem. A* **1999**, *103*, 5399–5408.

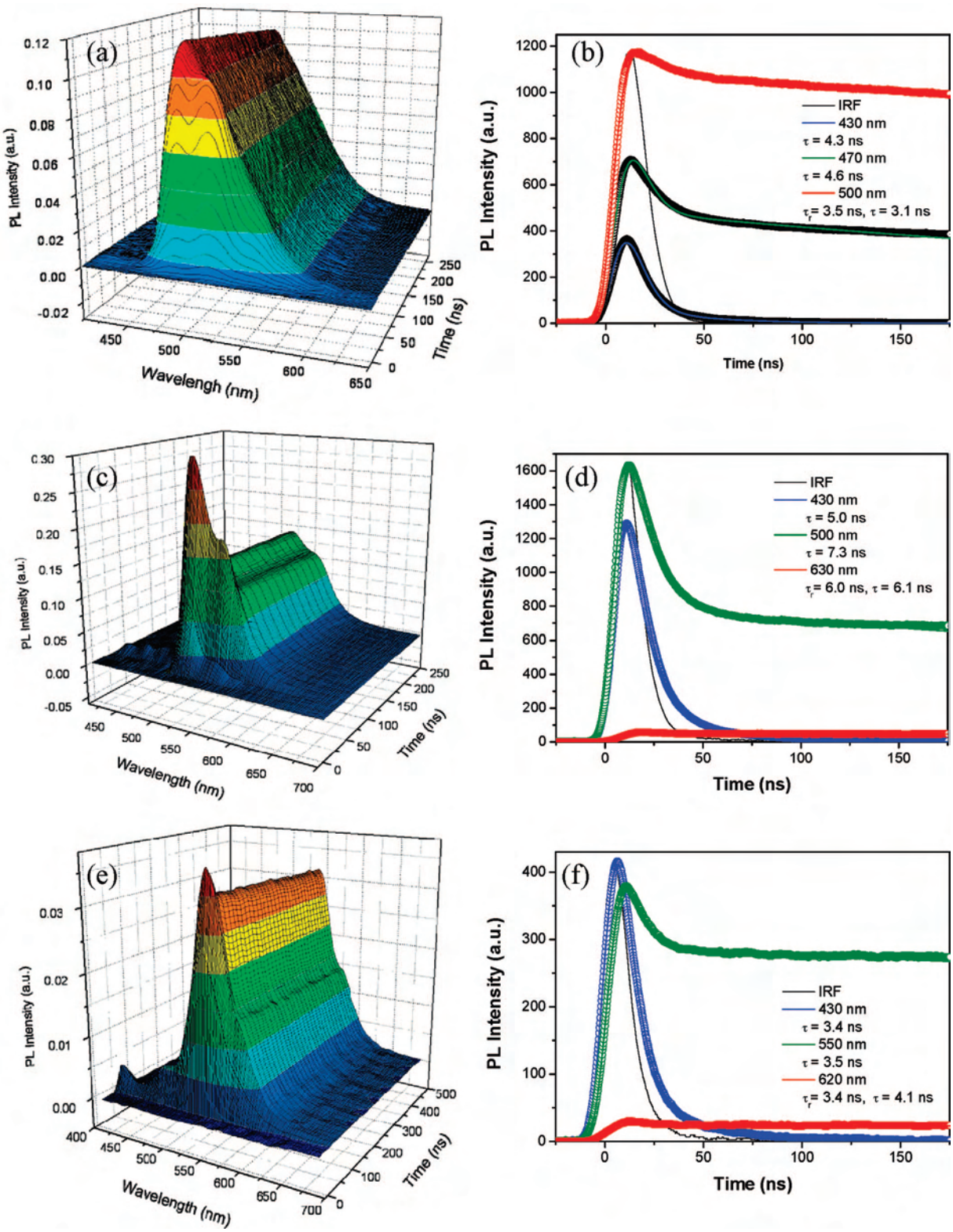

Figure 3. Evolution of transient photoluminescence spectra of **1** (a), **2** (c), and **3** (e), and the corresponding temporal decay profile of **1** (b), **2** (d), and **3** (f) in the solution state (1.0×10^{-5} M, Ar-saturated toluene; $\lambda_{excitation} = 355$ nm). For the transient photoluminescence spectra at a selected time, see the Supporting Information.

interligand energy transfer within the Ru/Os diads was observed to take place on the picosecond or sub-picosecond time scale.[25b,c] However, direct luminescent observations on the interligand energy transfer have been rarely reported for the case of ligands being coordinated to an identical metal center: for example, spectroscopic observations of excited-state ligand interaction have been reported for Ru(II) and Re(I) complexes bearing 2,2′-bipyridine and pyrene-appended bipyridine.[26]Additionally, interesting temperature-dependent dual emission behavior was reported for mixed

(26) Guerzo, A. D.; Leroy, S.; Fages, F.; Schmehl, R. H. *Inorg. Chem.* **2002**, *41*, 359–366.

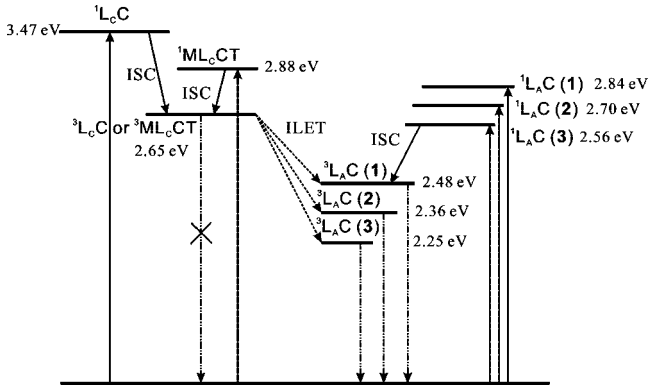

Figure 4. Schematic representation of the photophysical process involved in **1**–**3**.

chelates of Ir(III) comprising 2-phenylpyridine (ppy), benzo[*h*]quinoline (bzq), 1,10-phenanthroline (phen), or 2,2′-bipyridine (bpy), in which thermally assisted ILET from a higher energy MLCT state of the ppy or bzp ligand to a lower energy MLCT state of bpy or phen ligand was proposed.[27] However, in most cases, the energy transfer time scale between excited states, which are generated from different ligands, was not fully elucidated.[21,28] Thus, our observation of the interligand energy transfer time is to be considered important. While, at the present time, we do not understand clearly this rather slow ILET time scale, we can propose two possible reasons for this sluggish transfer: (1) poor electronic coupling between ligands across the core Ir atom and (2) large geometrical change which might be accompanied by the ILET. For the former case, it is anticipated that the existence of an Ir−O bond in the chromophoric ancillary ligand affords a low covalency to the bond which leads to weak electronic coupling with the cyclometalating ligand on the other side. However, DFT calculation results (Figure 2) reveal strong delocalization of the HOMO in both the phenolate of the ancillary ligand and Ir atom, thus precluding this possibility. In the case of the latter possibility, Watts et al. explained temperature-dependent dual phosphorescence from a heteroleptic Ir(III) complex comprising ppy and bpy ligands based on the internal geometry change which was possibly accompanied by energy transfer between them.[27] According to their explanation, a potential difference in the structure of the excited states before and after ILET might raise a necessary condition to overcome by the occurrence of rather slow relative nuclear displacements (Franck–Condon barrier). We consider that our Ir(III) complexes are basically similar to that series, and thus, the energy transfer time scale could be understood in a similar manner.

Another important thing which we have to consider is a possible Förster energy transfer from the cyclometalating ligand to the chromophoric ancillary ligand. If this Förster mechanism works, the ILET rate should be faster than those of previous Ir(III) complexes of the pyridylcarboxylate ancillary ligands because there was virtually no spectral overlap between ligands within the previous Ir(III) complex.[7d] However, it is observed that the ILET times (3–6 ns) of **1**−**3** are not significantly different from those (5–7 ns) of our previous publication. This observation most probably suggests that the ISC from the ^1L_CC state to the ^3L_CC state (or from the ^1ML_CCT state to the ^3ML_CCT state) is much faster than Förster energy transfer. Because it has been known that a spin–orbit coupling constant of Ir(III) is 50% larger than that of Ru(II),[19a] this enhanced ISC, and thus, our triplet ILET scheme might be the most probable reason for the relatively similar ILET time scale.

Overall, the excited energy flows down to the ^3L_CC (or ^3ML_CCT) state from the ^1L_CC and ^1ML_CCT state through facile ISC and followed by ILET with the time scale of ∼5 ns that is still faster than the emission lifetimes (>1 μs). This scheme enables us to maximize the efficiency (>99%) of ILET and to facilitate the ultimate color tunability with minimum energy loss. This novel scheme enlightens a new synthetic strategy to produce highly efficient OLEDs with variant color tunability. To summarize, highly efficient interligand energy-harvesting phosphorescence is achievable by utilizing the characteristic photophysical system with dual-mode excitation but a single-mode phosphorescence emission channel. The photophysical scheme based on collective data is schematically summarized in Figure 4.

As a final aspect of this study, we fabricated multilayer OLEDs. The OLED configuration is shown in Figure 5a, along with the energy levels of the component materials. In this study, generally used organic materials have been applied: indium tin oxide (ITO) on a glass substrate as the anode; copper(II) phthalocyanine (CuPc) as the hole-injecting material; 4,4′-bis[*N*-(1-naphthyl)-*N*-phenylamino] biphenyl (NPD) as the hole-transporting material; CBP as the host material; aluminum(III) bis(2-methyl-8-quinolinate)(4-phenylphenolate) (BAlq) as the hole-blocking layer; aluminum(III) tris(8-quinolinate) (Alq_3) as the electron-transporting material; and LiF/aluminum as the cathode. As summarized in Table 3, a maximum luminance of 9711 cd/m^2 and a maximum emission efficiency of 10.58 cd/A were recorded from the device based on **3**. The luminance and emission efficiency of the devices based on **1** and **2** were significantly inferior to those of the device containing **3**.[29] Interestingly, we found that the turn-on and driving voltages (at 10 mA/cm^2) increased as the oxidation potential of the Ir(III) complexes was lowered. This suggests that the holes from

(27) (a) King, K. A.; Watts, R. J. *J. Am. Chem. Soc.* **1987**, *109*, 1589–1590. (b) Ohsawa, Y.; Sprouse, S.; King, K. A.; DeArmond, M. K.; Hanck, K. W.; Watts, R. J. *J. Phys. Chem.* **1987**, *91*, 1047–1054.

(28) (a) Wilkinson, A. J.; Puschmann, H.; Howard, J. A. K.; Foster, C. E.; Williams, J. A. G. *Inorg. Chem.* **2006**, *45*, 8685–8699. (b) Yip, J. H. K.; Suwarno; Vittal, J. J. *Inorg. Chem.* **2000**, *39*, 3537–3543. (c) Chang, C.-J.; Yang, C.-H.; Chen, K.; Chi, Y.; Shu, C.-F.; Ho M.-L.; Yeh, Y.-S.; Chou, P.-T. *Dalton Trans.* **2007**, 1881–1890. (d) Bolink, H. J.; Cappelli, L.; Coronado, E.; Grätzel, M.; Ortí, E.; Costa, R. D.; Viruela, P. M.; Nazeeruddin, M. K. *J. Am. Chem. Soc.* **2006**, *128*, 14786–14787. (e) Burt, J. A.; Crosby, G. A. *Chem. Phys. Lett.* **1994**, *220*, 493–496. (f) Yeh, Y.-S.; Cheng, Y.-M.; Chou, P.-T.; Lee, G.-H.; Yang, C.-H.; Chi, Y.; Shu, C.-F.; Wang, C.-H. *ChemPhysChem* **2006**, *7*, 2294–2297.

(29) At present, the relatively low OLED efficiencies of **1** and **2** are thought to originate from poor locating of an exciton formation zone within the emitting layer of our preliminary OLEDs. See the electroluminescence spectra of **1** and **2** largely contaminated by NPD emission.

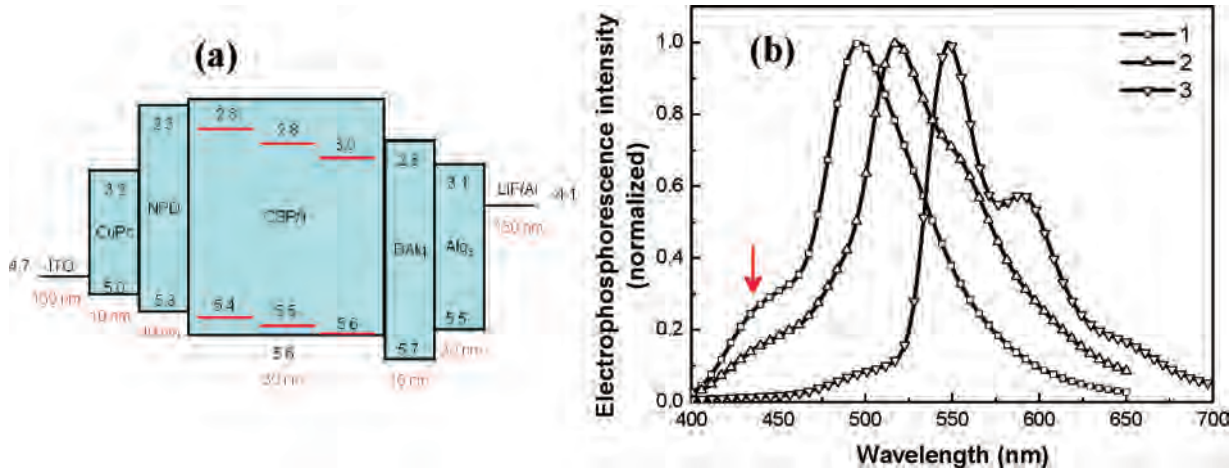

Figure 5. (a) Device configuration of OLEDs and the corresponding energy levels (eV) of the materials used. For the Ir(III) complexes, the values from left to right are for **1**, **2**, and **3**, respectively. (b) Electrophosphorescence spectra of the Ir(III) complexes (8 wt % doped) under 10 mA/cm^2.

Table 3. Electroluminescence Properties[a] of the Ir(III) Complexes

	λ_{max} (nm)	CIE	turn-on voltage (V)	driving voltage at 10 mA/cm^2 (V)	maximum luminance (cd/m^2)	maximum EQE (%)	maximum emission efficiency (cd/A)	maximum power efficiency (lm/W)
1	495	(0.20, 0.41)	3.6	8.7	3739	1.29	1.86	0.61
2	515	(0.28, 0.52)	3.8	9.5	4753	1.05	3.32	1.60
3	550	(0.42, 0.55)	3.8	9.2	9711	2.17	10.58	4.76

[a] Device configuration: ITO/CuPc (10 nm)/NPD (40 nm)/Ir (8 wt %):CBP (30 nm)/BAlq (10 nm)/Alq_3 (30 nm)/LiF:Al (150 nm).

the hole-transporting layer (NPD) may be transferred directly to the Ir(III) complexes rather than to the HOMO of CBP. The $J-V-L$ (current density–voltage−luminance) profiles of **1**−**3** and doping ratio dependency of the $J-V-L$ profiles for **3** are shown in the Supporting Information. The electrophosphorescence spectra of the Ir(III) complexes are the same as the phosphorescence spectra in Figure 1b but with contamination by an NPD emission (red arrow in Figure 5b),[30] indicating that this device structure needs further optimization. Importantly, however, the present experiments show that the characteristic phosphorescence mechanism also operates under electrical excitation to give the exclusive chromophoric ancillary ligand-centered phosphorescence. Hence, the proposed color tuning method should be applicable to practical OLEDs.

Summary

We have demonstrated a controlled phosphorescence color tuning in a series of heteroleptic Ir(III) complexes containing chromophoric 2-(2-hydroxyphenyl)oxazole-derivative ancillary ligands. From a cyclometalated chloride-bridged Ir(III) dimer, three highly emissive cyclometalated heteroleptic Ir(III) complexes were obtained in good yields. The three Ir(III) complexes showed highly efficient greenish blue (500 nm), green (525 nm), and yellow (552 nm) phosphorescence, respectively; a regular ca. 0.11 eV bathochromic shift was observed for each additional phenyl ring fused to the oxazole ring in the ancillary ligand. From the absorption spectra, electrochemical measurements, static and transient PL data, and TD-DFT calculations, it can be concluded that the Ir(III) complexes have a single emission center with dual excitation paths, thus facilitating interligand energy-harvesting phosphorescence. Finally, we demonstrated this characteristic energy harvesting phosphorescence in electrophosphorescence devices.

Acknowledgment. This work was supported by the Korea Science and Engineering Foundation (KOSEF) through the National Research Lab. The program was funded by the Ministry of Science and Technology (No. 2006-03246). The work at Yonsei University was financially supported by the Star Faculty Program of the Ministry of Education and Human resources. K.S.K. acknowledges the fellowship of the BK21 program from the MEHRD of Korea.

Supporting Information Available: Cyclic voltammograms, phosphorescence spectra of the film states, photoexcitation spectra, a plot of phosphorescence peak maxima as a function of solvent polarity parameter, and transient photoluminescence spectra of the Ir(III) complexes, current density versus voltage profiles as well as luminance, emission efficiency, and power efficiency profiles versus current density. This material is available free of charge via the Internet at http://pubs.acs.org.

IC701778F

(30) See the following reference for the electroluminescence spectrum of NPD Zhao, D. W.; Zhang, F. J.; Song, S. F.; Xu, C.; Xu, Z. *Appl. Surf. Sci.* **2007**, *253*, 7412–7415.